Shifts from pulled to pushed range expansions caused by reduction of landscape connectedness

Authors

Maxime Dahirel[1], Aline Bertin[1], Marjorie Haond[1], Aurélie Blin[1], Eric Lombaert[1], Vincent Calcagno[1], Simon Fellous[2], Ludovic Mailleret[1,3], Thibaut Malausa[1], Elodie Vercken[1]

[1]Université Côte d'Azur, INRAE, CNRS, ISA, France

[2]CBGP, INRAE, CIRAD, IRD, Montpellier SupAgro, Univ Montpellier, Montpellier, France

[3]Université Côte d'Azur, INRIA, INRAE, CNRS, Sorbonne Université, BIOCORE, Sophia Antipolis, France

Corresponding author: MD, maxime.dahirel@yahoo.fr

Abstract

Range expansions are key processes shaping the distribution of species; their ecological and evolutionary dynamics have become especially relevant today, as human influence reshapes ecosystems worldwide. Many attempts to explain and predict these phenomena assume, explicitly or implicitly, so-called "pulled" expansion dynamics, in which the low-density edge populations provide most of the "fuel" for the species advance. Some expansions, however, exhibit very different dynamics, with high-density populations behind the front "pushing" the expansion forward. These two types of expansions are predicted to have different effects on factors such as genetic diversity and habitat quality sensitivity. However, studies are lacking due to the challenge of generating reliably pushed vs. pulled expansions in the laboratory, or discriminating them in the field. We here propose that manipulating the degree of structural connectivity (connectedness) among populations may prove a more generalizable way to create pushed expansions. We demonstrate this with both individual-based simulations as well as replicated experimental range expansions (using the parasitoid wasp *Trichogramma brassicae* as model). By analysing expansion velocities and neutral genetic diversity, we showed that reducing connectedness led to pushed dynamics. Our numerical and experimental results suggest that reducing connectedness can cause density-dependent spread (and thus pushed range expansions) both directly or by amplifying existing density-dependence. In the current context of habitat loss and fragmentation, we need to better account for this relationship between connectedness and expansion regimes to successfully predict the ecological and evolutionary consequences of range expansions.

Keywords biological control, biological invasions, density-dependent dispersal, individual-based model, range shifts, *Trichogramma*

Introduction

Range expansions and range shifts into novel habitats and landscapes are key ecological processes shaping the abundance and distribution of species (Sexton, McIntyre, Angert, & Rice, 2009). Understanding their ecological and evolutionary drivers and consequences has become especially relevant in the context of more frequent biological invasions (Facon et al., 2006; Renault, Laparie, McCauley, & Bonte, 2018) or increasing impacts of climate change (Hill, Griffiths, & Thomas, 2011; Lavergne, Mouquet, Thuiller, & Ronce, 2010; Parmesan, 2006).

Range expansions are usually modelled and analysed in a framework based on the Fisher-KPP partial differential equation and its numerous declinations (see e.g. Hastings et al., 2005; Lewis, Petrovskii, & Potts, 2016). In this framework, range dynamics generally converge to solutions of constant profiles moving in space at a fixed velocity, called travelling waves. Travelling waves are considered "pulled" when spread is driven mostly, if not only, by the dynamics at the leading edge of the expansion. In biological range expansions, this happens when growth and dispersal rates are maximal at low densities; the velocity of the wave then only depends on low-density dispersal and growth (e.g. Birzu, Matin, Hallatschek, & Korolev, 2019). While growth and dispersal functions that are expected to generate pulled expansions certainly happen in nature (Harman, Ii, Shivaji, & Cronin, 2020; Matthysen, 2005; Williams & Levine, 2018), they are not the only ones possible. For instance, growth rates can be reduced at low densities compared to intermediate ones, a phenomenon known as the Allee effect (Berec, Angulo, & Courchamp, 2007). Additionally, dispersal is often maximised at high densities (positive density-dependence) as it provides a mechanism to escape increased competition (Bowler & Benton, 2005; Harman et al., 2020; Matthysen, 2005). In both cases, we would expect the advance of the expansion to be driven not by the low-density front populations, but by the population dynamics in a region located behind the front, where growth and/or dispersal are maximal. These "pushed" waves (Stokes, 1976) behave very differently than pulled waves (see e.g. Lewis et al., 2016). They will typically advance faster than expected based solely on growth and dispersal rates observed at low densities (i.e. in edge patches) (see e.g. Gandhi, Korolev, & Gore, 2019). The ratio of the actual expansion velocity v to the velocity v_F expected for a pulled expansion with the same low-density behaviour has been proposed as a quantitative indicator discriminating pulled, "semi-pushed" and pushed expansions (e.g. Birzu, Hallatschek, & Korolev, 2018). This ratio has been connected to other key metrics expected to vary along the pushed/pulled gradient (Birzu et al., 2018). In the context of biological range expansions or shifts, this includes the rate at which the front of the expansion loses genetic diversity due to drift and successive founding events as it advances. Indeed, models and experiments show that neutral genetic diversity is lost at the expanding edge much more slowly in pushed than in pulled expansions (Birzu et al., 2018, 2019;

Gandhi et al., 2019; Hallatschek & Nelson, 2008; Roques, Garnier, Hamel, & Klein, 2012), with estimated times to allele fixation differing by up to several orders of magnitude (Gandhi et al., 2019).

A key challenge for empirically studying the ecological and evolutionary consequences of pushed and pulled expansions (which, besides neutral genetic diversity, remain poorly known; see discussion in Birzu et al., 2019) is to obtain comparable expansions known to be either pushed or pulled. One could contrast strains, populations or closely related species naturally differing in the intensity of density-dependent dispersal and/or Allee effects (Harman et al., 2020; Jacob, Chaine, Huet, Clobert, & Legrand, 2019; Matthysen, 2005; Walter, Grayson, Blackburn, Tobin, & Johnson, 2019). However, they are likely to also differ in other key traits (Jacob et al., 2019), making direct comparisons difficult. A better experimental solution would be to manipulate the focal species/population/strain's environment to change the presence or strength of Allee effects and/or density-dependent dispersal. For instance, Gandhi et al. (2019; 2016) managed to reliably produce pushed expansions by changing the substrate on which *Saccharomyces cerevisiae* yeasts were grown: while yeasts grow best at low densities on monosaccharides, they present an Allee effect when they have to use a disaccharide like sucrose. Externally manipulating density-dependent dispersal may be more difficult, but could conceivably also be done by changing the resource (Endriss et al., 2019; Kuefler, Avgar, & Fryxell, 2012; Van Allen & Bhavsar, 2014). Adding or removing conspecific cues independently of actual population size may also be an option (De Meester & Bonte, 2010), but not all organisms have resources or cues that are easy and useful to manipulate experimentally (Fellous, Duncan, Coulon, & Kaltz, 2012).

Rather than manipulating the within-patch conditions, another solution that may be more generalizable would be to reduce the level of connectedness, that is the number, length or quality of the physical links between patches/populations (i.e. structural connectivity; Baudry & Merriam, 1987). We hypothesize such experimental manipulations could lead to increased positive density-dependent spread, and thus more pushed expansions, because of dispersal stochasticity. Indeed, at low population sizes, reducing the dispersal rate by limiting connectedness sharply increases the risk populations at the edge of the expansion will fail to send any disperser, due to stochasticity alone (**Fig. 1**). This can increase the influence of population density on dispersal success, leading to pushed expansions. This effect may only occur when populations at the very edge of the expansions are of few individuals, typically less than a hundred (Fig. 1). Such edge population densities are probably not uncommon in some taxonomic groups, where core population sizes are in the 100-1000 range (Krauss, Steffan-Dewenter, & Tscharntke, 2003; Santini, Isaac, & Ficetola, 2018). They are however much lower than those considered in most pushed expansion models and experiments (tens to hundreds of thousands individuals per patch; e.g. Birzu et al., 2018; Gandhi et al., 2019), which may

explain why the possible effects of reduced connectedness have been overlooked so far. Besides, models have often assumed continuous population densities instead of discrete individuals, which prevent the density-dependence described in **Fig. 1** from occurring (as discussed in Pachepsky & Levine, 2011). An indication that reducing connectedness may work and generate pushed expansions can be found in an earlier simulation study by Morel-Journel et al. (2016). In that study, increasing the level of dispersal stochasticity led to levels of within-landscape population variability more closely resembling simulated pushed expansions than pulled ones.

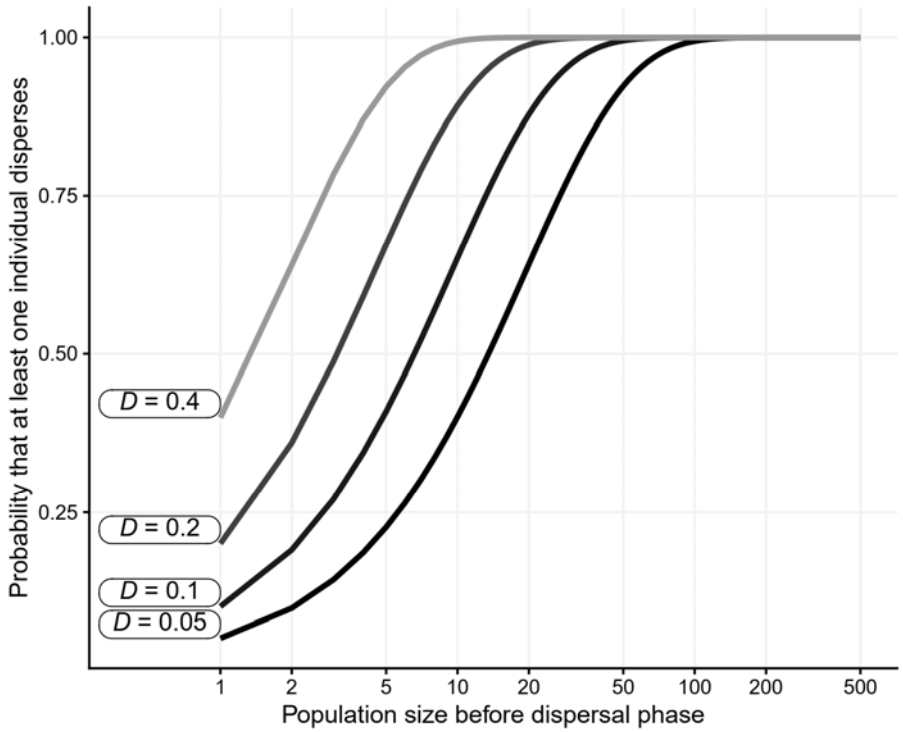

Figure 1. Probability that at least one individual disperses from a patch (Pr(n>0)) as a function of its population size N pre-dispersal and average dispersal rate D. Dispersal stochasticity is obtained by assuming the number of dispersers n from a patch is drawn from a Binomial distribution n=Binom(N,D). Note the log scale on the x-axis.

In the present study, we aimed to demonstrate, combining simulations and experimental approaches, that (more) pushed expansions can indeed arise from reductions of habitat connectedness, at population densities that are realistic for many "macroscopic" organisms (Krauss et al., 2003; Santini et al., 2018). In individual-based simulations, we examined expansion velocities and the dynamics of neutral genetic diversity to (a) confirm Allee effects and density-dependent dispersal (Birzu et al., 2019) still lead to pushed expansions at "low" equilibrium population sizes K, and (b) show that reducing connectedness (by decreasing effective dispersal rates) can also generate

pushed fronts even in the absence of the other two mechanisms. We complemented this approach by using minute wasps of the genus *Trichogramma* (Haond et al., 2018; Morel-Journel et al., 2016) in replicated experimental landscapes (Larsen & Hargreaves, 2020), to investigate whether reduced connectedness influenced the velocity and neutral genetic dynamics of "real" range expansions.

Methods

Simulations

To determine whether the new mechanism we propose, reduced connectedness, can actually generate pushed expansions, we used an individual-based model (IBM) approach (DeAngelis & Mooij, 2005 for a review). The model is in discrete time and space and simulates the dynamics of a haploid clonal species with non-overlapping generations, expanding in one direction in a one-dimensional landscape. Range expansions unfold during 100 generations in a landscape long enough that they never run out of empty patches. In practice, given the expansions advance in only one direction and individuals can only disperse at most one patch per generation (see below), this means any landscape length higher than the number of generations. All patches are of equal and constant quality, determined by the equilibrium population density *K*. In the present study, we studied two *K,* 225 and 450, as the relationship between *K* and the expansion velocity *v* is expected to differ between pushed and pulled expansions (Haond et al., 2018). These densities are within the range of *K* used in Haond et al. (2018)'s simulations, and correspond respectively to 50% and 100% of the largest possible population in our experimental expansions (see below).

At the start of the expansion, *K* adult individuals that have not yet reproduced are introduced in one patch at one of the two extremities of the landscape (coordinate $x = 0$). To be able to later study genetic diversity, all individuals are randomly assigned one of two allele values (coded 0 and 1) at a neutral genetic locus *L*. Each generation until the end of a run, the life cycle then happens as follows:

(1) Adult individuals disperse with a probability $D = logit^{-1}\left(logit(D_0) + \beta_{density} \times {}^{N}/_{K}\right)$, where D_0 is the (hypothetical) dispersal rate at $N = 0$, $\beta_{density}$ the slope of the dispersal-density relationship on the logit scale, and *N* the patch population size immediately before the dispersal phase. This function is based on the way empirical dispersal-density data are usually analysed (through generalized linear models; see e.g. Marjamäki, Contasti, Coulson, & McLoughlin, 2013). Dispersers randomly move to one of the nearest neighbouring patches; that is, the maximal dispersal distance is of 1 patch.

(2) Individuals then produce F offspring, with $F \sim \mathrm{Poisson}(\lambda)$ and λ based on a Ricker equation modified to allow potential Allee effects (Morel-Journel et al., 2016): $\lambda = e^{r_0(1-N/K)(1-A/N)}$ where r_0 is the hypothetical expected growth rate at $N = 0$ in the absence of Allee effects, and A an Allee threshold such that $A = 0$ leads to no Allee effects, $0<A\leq 1$ leads to weak Allee effects (*sensu* e.g. Berec et al., 2007, i.e. where positive density-dependent growth never leads to negative growth rates), and $A > 1$ leads to strong Allee effects (where growth rates are negative for $N < A$). All new individuals inherit the value at the neutral locus L from their parent with no mutation.

(3) All adults die; juveniles then become adults.

The model was written in Netlogo (Wilensky, 1999), version 6.1.1, and set up using the *nlrx* R package (Salecker, Sciaini, Meyer, & Wiegand, 2019). We tested 4 scenarios (× 2 possible values of K; see **Table 1**). The "reference" scenario had no Allee effects, no density-dependent dispersal ($\beta_{density} = 0$) and a dispersal rate D_0 set to 0.2, a biologically plausible rate according to many experimental (e.g. Fronhofer et al., 2018) or natural observations (Marjamäki et al., 2013; Stevens et al., 2013). The three other scenarios, which we expected to lead to pushed expansions, each differed from the reference by one parameter: either a weak Allee effect was present ($A = 0.95$), there was positive-density-dependent dispersal ($\beta_{density} = 1$) or connectivity was reduced by half ($D_0 = 0.1$). In all cases r_0 was set to ln(5), a value chosen to be biologically plausible (Cerutti & Bigler, 1995) and to keep computing times reasonable. Each scenario was replicated 100 times.

Table 1: Values of key parameters of the individual-based model used to simulate range expansions, for the four scenarios considered in the present study. Values that differ from the reference are in **bold**.

Parameter name and description	Value in scenario :			
	reference	density-dependent dispersal	(weak) Allee effect	reduced connectivity
K : equilibrium population size	225 or 450	225 or 450	225 or 450	225 or 450
r_0: growth rate at N = 0 (in the absence of Allee effects)	ln(5)	ln(5)	ln(5)	ln(5)
D_0: dispersal rate at N = 0	0.2	0.2	0.2	**0.1**
$\beta_{density}$: slope of the dispersal-density relationship (logit scale)	0	**1**	0	0
A : Allee effect parameter	0	0	**0.95**	0

Experimental range expansions

We used laboratory strains of the haplo-diploid egg parasitoid *Trichogramma brassicae* Bezdenko, 1968 (Hymenoptera: Trichogrammatidae) as our model in experiments (**Supplementary Material 1**). *T. brassicae* wasps are raised routinely in the lab using eggs of the Mediterranean flour moth *Ephestia kuehniella* Zeller 1879 (Lepidoptera: Pyralidae) as substitution host. *E. kuehniella* eggs are irradiated before use, which prevents their larval development while still allowing *Trichogramma* wasps to use them as hosts (St-Onge, Cormier, Todorova, & Lucas, 2014). To be able to better generalize our results, we used three independent genetic mixes of *T. brassicae* (**Supplementary Material 1**). Note that the effect of genetic background itself is not the object of the present manuscript, and is thus not analyzed directly in any of our statistical models, for simplicity (as in Van Petegem et al., 2018).

To experimentally test the effects of reduced connectivity on range expansions, we set up a series of one-dimensional artificial landscapes in which we monitored *T. brassicae* wasps for 14 non-overlapping generations (including initially released adults, i.e. generation 0). The landscapes were made of closed plastic vials (5 cm diameter, 10 cm height) connected by either two ("reference"-level connectedness) or one (reduced connectedness) flexible tubes to each of their nearest neighbours (tube length: 40 cm, internal diameter: 5 mm). Landscapes were initially 4 patches long, to allow dispersal kernels with movements > 1 patch, and extended as needed to ensure there were always at least 2 available empty patches beyond the current front. Each treatment was replicated 12 times (4 per genetic mix), for a total of 24 experimental landscapes. Landscapes were initiated by introducing ≈ 300 adult wasps (range 261 – 324) in one extremity patch (coordinate x = 0), so the expansion could only advance in one direction in each landscape. Landscapes were kept under standardized conditions (23°C, 70% relative humidity, 16:8 L:D). Each generation then unfolded along the following steps:

- (a) We provided approximately 450 new eggs of *Ephestia kuehniella* per patch for wasps to lay eggs in. *E. kuehniella* eggs were presented on paper strips to facilitate handling.

- (b) Adults (and old egg strips) were removed after 48 hours to enforce non-overlapping generations and standardized generation times.

- (c) When parasitoid larval development was advanced enough to identify signs of parasitism (host eggs darkening after ≈7 days), we temporarily removed egg strips from patches and assessed the presence/ absence of parasitized eggs by eye. We also photographed all patches with parasitized

eggs for semi-automatic estimations of population sizes (Nikon D750 60mm f/2.8D macro lens, 24.3 Mpix, **Supplementary Material 2**). Eggs were then replaced in their patches until the emergence of the first adults, when we started a new cycle from step (a).

We estimated the reduction of connectivity imposed by the experimental design by comparing the estimated mean egg-laying distances (in patches from release sites) between treatments at the start of the experiment, i.e. the only time point when the source patch of all egg-laying individuals was known. The average egg-laying distance was reduced by ≈ 25% in "reduced connectedness" landscapes compared to "reference" ones (**Supplementary Material 2 and 3**).

Microsatellite genotyping (experimental expansions)

To determine how genetic diversity evolved during experimental range expansions and whether it was influenced by connectedness, we kept and genotyped adult female wasps after their removal from the experimental landscapes. In each landscape, we sampled initially released individuals (i.e. generation 0; hereafter "origin" wasps) as well as wasps found in both the release patch (hereafter "core" wasps) and the most advanced population ("edge" wasps) at generations 4, 8 and 12. In each patch × time combination, we aimed to sample about 20 individuals; the actual number was sometimes lower especially in edge populations with fewer individuals (average ± SD: 18.10 ± 2.63 wasps; range: 4-28; total: 3043). Wasps were genotyped at 19 microsatellite loci; their characteristics, as well as the DNA extraction and amplification protocols, are detailed in **Supplementary Material 4.**

Statistical analyses

All data (experimental and simulated) were analyzed in a Bayesian framework, using R, version 4.0.2 (R Core Team, 2020) and the *brms* package version 2.11.1 (Bürkner, 2017) as frontends to the Stan language (RStan version 2.19.2; Carpenter et al., 2017; Stan Development Team, 2018). We used nonlinear multilevel/mixed models. The model descriptions below are summaries aiming for clarity rather than completeness; formal and complete write-ups for all statistical models are given in **Supplementary Material 5**. We use general-purpose "weakly informative" priors based on McElreath (2020) for all parameters except one where there is strong theoretical prior knowledge (see **Supplementary Material 5**). For each model, we ran four chains with enough iterations to ensure effective sizes were satisfactory for all fixed effect, random effect and distributional parameters (both bulk- and tail-ESS *sensu* Vehtari, Gelman, Simpson, Carpenter, & Bürkner, 2020 > 1000). In addition to graphical posterior checks (Gabry, Simpson, Vehtari, Betancourt, & Gelman, 2019; Vehtari et al., 2020), we checked chain convergence using the improved $\widehat{R}$ statistic by Vehtari et al. (2020).

All credible intervals given in text and figures are Higher posterior Density Intervals (HDIs). Data handling and figure generation were mainly done using the various *tidyverse* packages (Wickham et al., 2019), as well as the *tidybayes* (Kay, 2019) and *patchwork* (Pedersen, 2019) packages.

<u>- Expansion velocity</u>

In the long run, the position X_t of the front (i.e. the distance between the farthest populated patch and the release site) is expected to increase linearly with time t, whether expansions are pushed or pulled (e.g. Lewis et al., 2016):

$$X_t = v\,t$$

, where v is the asymptotic expansion velocity. However, expansions only settle on the velocity v after a transition period; the above equation is likely ill-suited for estimating front positions when expansions are followed during their early stages and population sizes are low (so stochasticity is high). In these cases, which correspond to the present study, we propose to use the following model:

$$X_t = v_t t$$

$$v_t = v + (v_1 - v) \times e^{-\lambda_{[v]}\,(t-1)}$$

, where v_1 is the initial velocity after 1 generation of expansion (we use v_1 as our "starting point", and thus t – 1, because estimating velocities at t = 0 leads to convergence problems), and $\lambda_{[v]}$ the rate of exponential convergence to the asymptotic velocity v.

We fitted this model to both simulated and experimental front locations, assuming a lognormal distribution to account for the fact distances travelled are always strictly positive. For experimental data, the submodels for $\ln(v_1)$, $\ln(v)$ and $\log_{10}(\lambda_{[v]})$ included fixed effects for treatment as well as random effects of replicate identity. For simulated data, we made three slight adjustments. First, we only used data from every fifth generation, to reduce computation time (by about an order of magnitude, based on preliminary tests) without significant impact on predictive success. Second, the submodel for v used logit(v) instead of $\ln(v)$, as velocities were by design ≤ 1 (due to nearest neighbour dispersal). Finally, the model was simplified by setting v_1 to 1; given the initial population size at t = 0, all simulated landscapes were all but guaranteed to send at least one individual to the next patch during the first generation, (see **Fig. 1**), leading to a velocity ≈ 1 patch/generation at t = 1.

In simulations, the growth and dispersal functions are fully known, so we were also able to directly compare the estimated v to their respective v_F, the predicted velocity for a pulled wave with the same D_0 and r_0 (Birzu et al., 2019; Lewis et al., 2016):

$$v_F = 2\sqrt{r_0 d_0}$$

, where d_0 = 0.5 D_0 for a one-dimensional landscape with nearest neighbour dispersal (see equation 7a in Birzu et al., 2019). Pulled expansions are expected to have $\frac{v}{v_F} = 1$ (with some stochastic fluctuations), fully pushed expansions to have $\frac{v}{v_F} \geq \frac{3}{2\sqrt{2}}$, and so-called semi-pushed expansions to be in-between (Birzu et al., 2018, 2019). Because the formula we use for Allee effects leads to a fecundity of 0 at density = 0, and because growth and dispersal at density = 0 are not meaningful anyway, we used r_1 and D_1 at N = 1 to estimate v_F rather than the "true" r_0 and D_0.

<u>- Genetic diversity, experimental data</u>

When expected heterozygosity (Nei, 1973) H is used as a measure of genetic diversity, theory predicts the genetic diversity both in core patches and at the edge of a range expansion should decay exponentially with time t (Birzu et al., 2018; Hallatschek & Nelson, 2008):

$$H_t \sim H_0 . e^{-\lambda_{[g]} t}$$

, where H_0 is the initial heterozygosity, and $\lambda_{[g]}$ the rate of decay of genetic diversity. For experimental data, we used this equation directly in a non-linear model to estimate whether the dynamics of genetic diversity varied between our two treatments and between core and edge patches. Multilocus expected heterozygosity was first calculated for each location (core/edge) × time combination using microsatellite data and the *adegenet* package (Jombart, 2008). Our submodel for $\lambda_{[g]}$ included fixed effects for treatment, location (initial release patch for "core"/ most advanced patch for "edge") and their interactions, as well as a random effect of replicate identity. The submodel for the initial diversity H_0 only included the random effect of replicate, as we did not expect differences between treatments beyond random fluctuations, and core/edge patches are the same at t = 0. Location was included in the $\lambda_{[g]}$ submodel as a centred dummy variable (-0.5 for "core", 0.5 for "edge") set to 0 at t = 0 as, again, core/edge patches are the same at t = 0. The submodels were estimated on logit(H_0) and $\log_{10}(\lambda_{[g]})$ to keep them within proper bounds; expected heterozygosities are proportions, and the decay rate $\lambda_{[g]}$ must be positive. We fitted the overall model on logit(H_t) using a Student t distribution, rather than on H_t using a Beta distribution (and a logit link). This is because the former is likely to be more robust to rare outliers (Kruschke, 2015), like those caused by sampling effects before genotyping (see companion script for detailed model comparisons, **Data availability**).

<u>- Genetic diversity, simulated data</u>

With simulated data, we cannot use the equation above as our basis to fit a model. This is because the way we simulate neutral genetic diversity (one locus with only two alleles in a haploid species) means values of H_t = 0 are very frequent (especially as t increases), and our previous model cannot be fitted to data containing zeroes. We instead used the fact that, with two alleles and if a given treatment is replicated a large number of times, a version of $\lambda_{[g]}$ can also be recovered from the way among-replicate variance in allelic frequencies V (for either allele) changes with time (Gandhi et al., 2019):

$$V_t \sim V_{max} \cdot (1 - e^{-\lambda_{[g]} t})$$

, where V_{max} is both the product of initial allelic frequencies and the asymptotic variance reached when all replicates have fixed one of the alleles. As for experimental data, our submodel for $\log_{10}(\lambda_{[g]})$ included fixed effects for treatment, location (core/edge) and their interactions. The submodel for logit(V_{max}) included only a constant intercept, as V_{max} should be identical between all cases (and ≈ 0.25) but for random sampling fluctuations. We fitted this model on all data with $t > 0$ using a Beta distribution, as the issues raised for experimental data above regarding outliers did not apply (each data point here being the summarized outcome of 100 independent populations).

Results

Expansion velocity

In simulations, absolute asymptotic expansion velocity v differed between treatments: density-dependent dispersal led to higher velocities than in reference expansions, while Allee effects and reduced connectivity led to slower expansions (**Fig. 2**, **Supplementary Material 6**). Regarding relative velocities $\frac{v}{v_F}$, reference landscapes were very close to speeds expected for pulled expansions (average velocity ratios $\frac{v}{v_F}$ = 1.01 and 0.98 for K = 450 and 225 respectively, **Fig. 2**); the other three treatments all had higher velocity ratios and were firmly in the range corresponding to pushed expansions (average velocity ratios $\frac{v}{v_F} \geq \frac{3}{2\sqrt{2}}$, **Fig. 2**). Expansions were faster when K = 450 than when K = 225 for all four treatments (**Fig. 2**, **Supplementary Material 6**).

In experiments, absolute estimated asymptotic velocities were virtually indistinguishable between reference and "reduced connectedness" landscapes (**Fig. 3**). Similar results were found with other model parameters such as the initial speed or the rate of convergence towards the asymptotic speed (**Supplementary Material 6**).

Shifts in genetic diversity

In simulations, genetic diversity declined faster, as measured by the decay rate λ, in edge patches than in core patches for all treatments (**Fig. 4**, **Supplementary Material 6**). In both core and edge patches, density-dependent dispersal and Allee effects led to a slower rate of diversity loss compared to the reference (**Fig. 4**, **Supplementary Material 6**). By contrast, reducing connectedness led to a faster rate of diversity loss (**Fig. 4**, **Supplementary Material 6**). In all four treatments and whether we looked at core or edge patches, genetic diversity was lost faster when K = 225 than when K = 450 (**Fig. 4**, **Supplementary Material 6**).

In the experimental landscapes, genetic diversity also decayed on average in all tested contexts of our experiment (**Fig. 5**), and we also found differences between edge and core patches and between both treatments. The rate of genetic diversity loss did not differ clearly between treatments in core patches (mean $\Delta_{\text{reference-reduced}} = -6.51 \times 10^{-3}$, 95% CI : [$-14.70 \times 10^{-3}$, 2.38×10^{-3}]), but diversity was lost more rapidly in reference edge patches than in "reduced connectedness" ones (mean $\Delta_{\text{reference-reduced}} = 18.30 \times 10^{-3}$, 95% CI : [$1.96 \times 10^{-3}$, 35.80×10^{-3}]) (**Fig. 5**, **Supplementary Material 6**). In addition, while edge patches lost diversity faster than core patches in reference landscapes, (mean $\Delta_{\text{edge-core}} = 40.5 \times 10^{-3}$, 95% CI : [$27.5 \times 10^{-3}$, 53.8×10^{-3}]), this difference was still present but reduced when connectedness was reduced (mean $\Delta_{\text{edge-core}} = 15.7 \times 10^{-3}$, 95% CI : [$8.15 \times 10^{-3}$, 24.3×10^{-3}]) (**Fig. 5**).

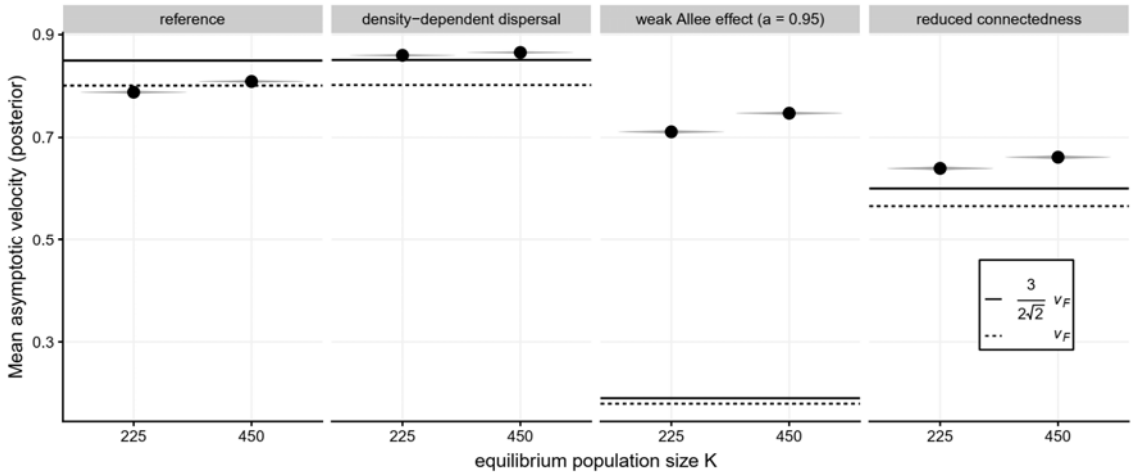

Figure 2. Posterior distribution of the average asymptotic expansion velocity (v) in simulations, depending on simulation scenario and equilibrium population size K (dots: posterior means). The horizontal lines mark the range between $\frac{v}{v_F} = 1$ (i.e. pulled expansions) and $\frac{v}{v_F} = \frac{3}{2\sqrt{2}}$ (limit between semi-pushed and fully pushed expansions; Birzu et al., 2018, 2019).

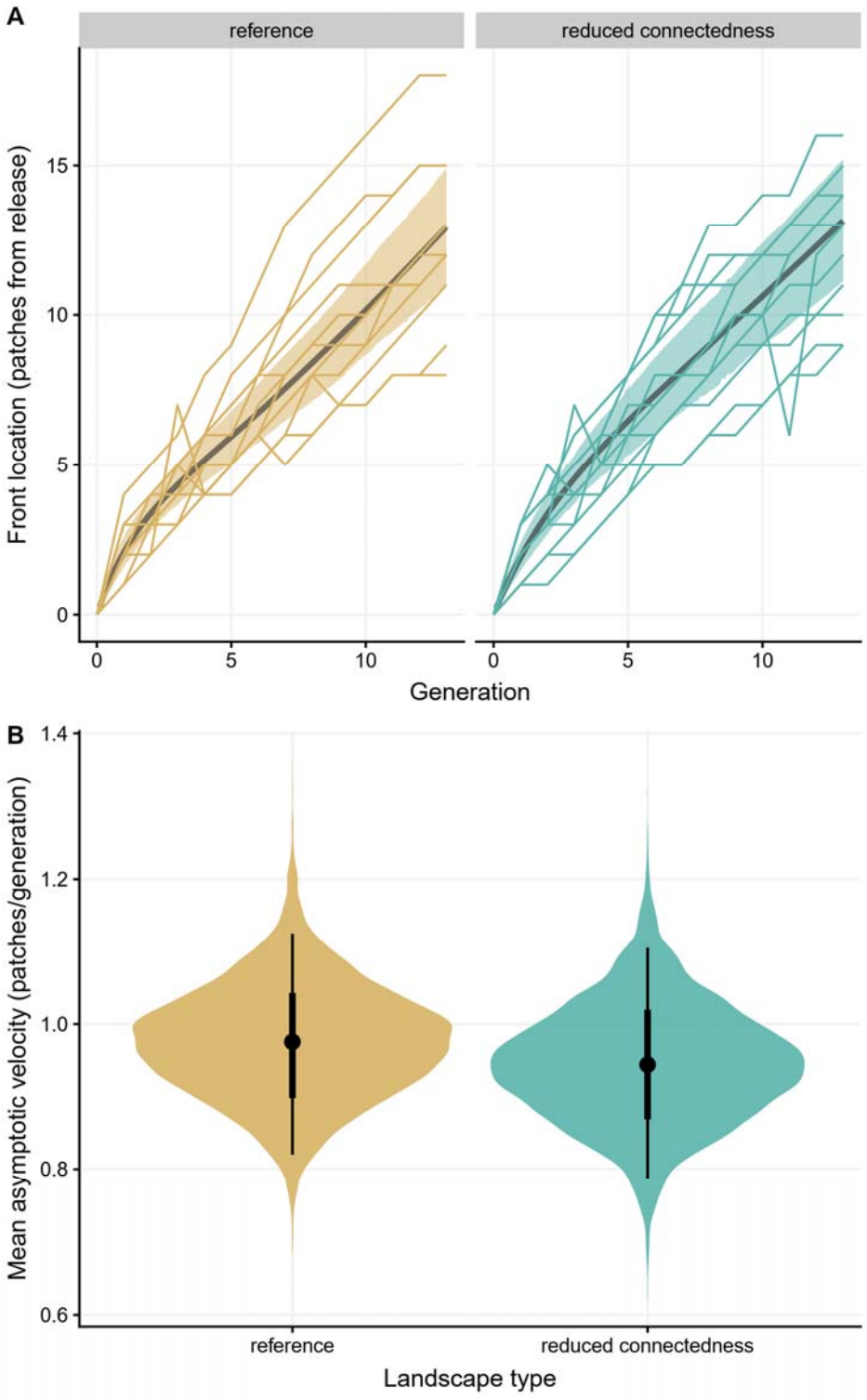

Figure 3. (A) Front locations as a function of the number of generations since release and experimental landscape type. Posterior means and 95% credible bands are displayed along observed trajectories for each landscape. (B) Posterior average asymptotic velocity *v* as a function of landscape type. Dots are posterior means, vertical bars 66 and 95% credible intervals.

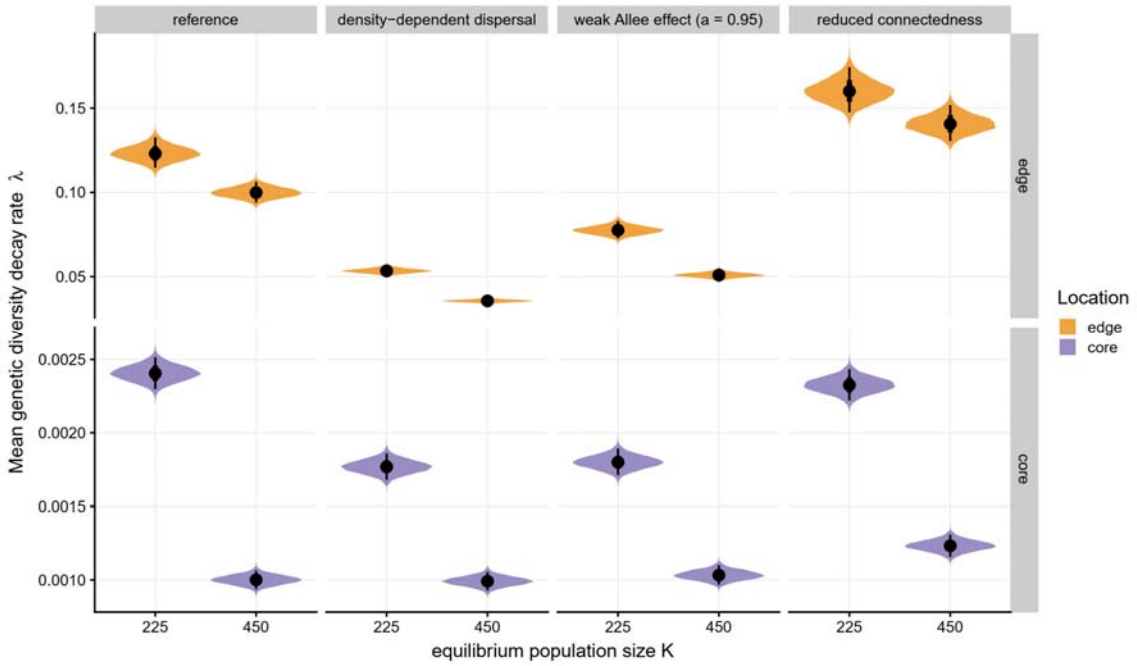

Figure 4. Posterior distribution of the average decay rate of genetic diversity with time (λ) in simulations, depending on simulation scenario, equilibrium population size K and patch location (either the original release site (core) or the most advanced patch at the time of measure (edge)). Dots are posterior means, vertical bars 95% credible intervals. Please note that posteriors for core and edge patches are displayed on different scales on the y-axis, for readability.

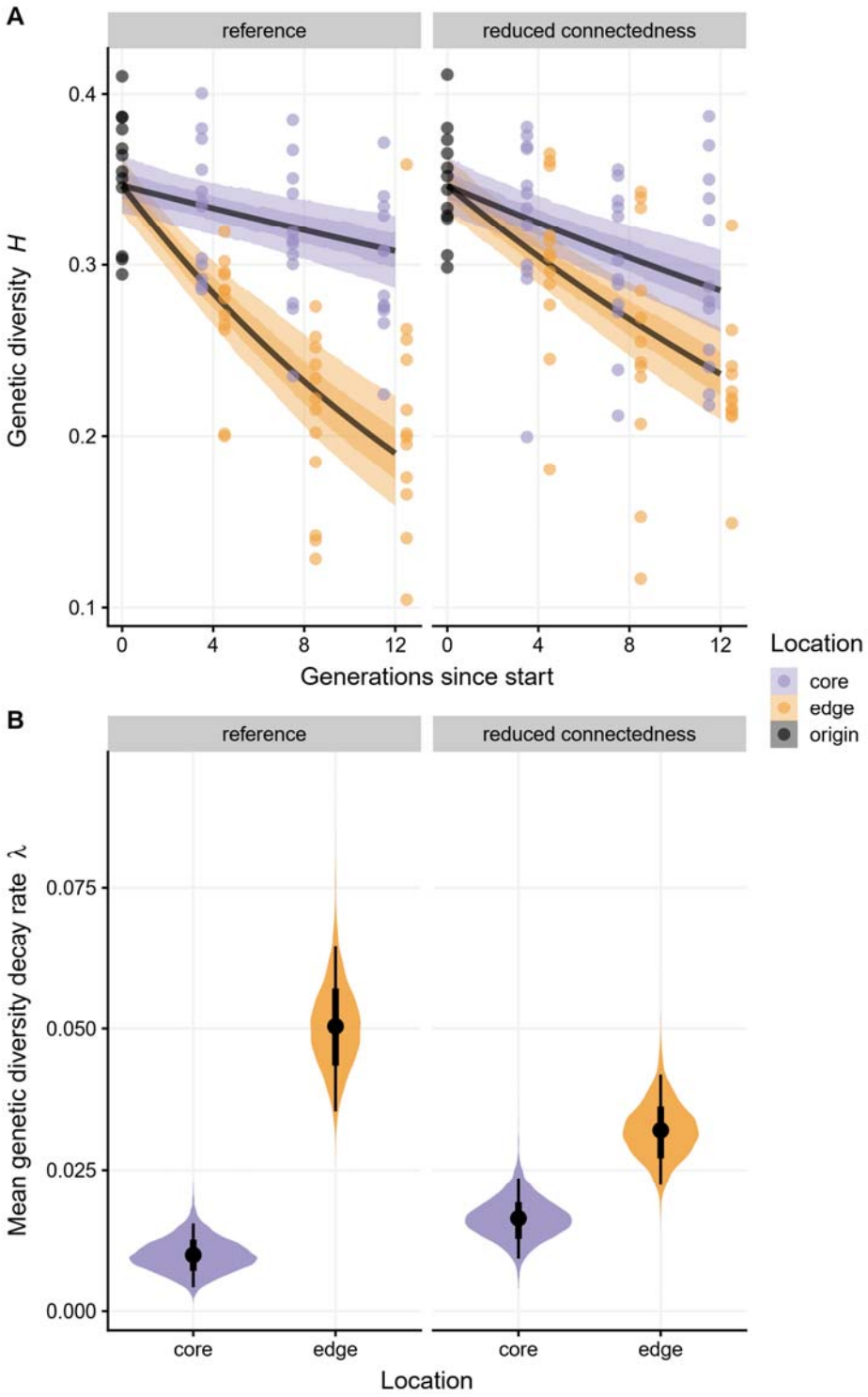

353

354 **Figure 5.** (A) Observed (points) and predicted (lines and bands) genetic diversity as a function of
355 generations since release and landscape type. For predictions, lines are the posterior means and
356 bands correspond to the 66/95% credible intervals. (B) Posterior distribution of the average genetic
357 diversity decay rate λ as a function of landscape type and patch location (either the original release
358 site (core) or the most advanced patch at the time of measure (edge)). Dots are posterior means,
359 vertical bars 66 and 95% credible intervals.

Discussion

By combining an individual-based model and replicated range expansions in experimental landscapes, we showed that reducing connectedness can lead to more pushed expansions. Discrepancies between the simulation and experimental results, as well as comparisons between the different simulation treatments, potentially shed light on the mechanisms at play in each context.

<u>Expansion velocity as a quantitative and qualitative indicator of pushed expansions</u>

First, our simulation results largely confirm previous theoretical and empirical results regarding the effects of density-dependent dispersal and Allee effects (Birzu et al., 2018, 2019; Gandhi et al., 2019, 2016; Hallatschek & Nelson, 2008; Roques et al., 2012). We show that both mechanisms lead to expansions that can be classified as "pushed" based on the velocity ratio ($\frac{v}{v_F} \geq \frac{3}{2\sqrt{2}}$; following Birzu et al., 2018, **Fig. 2**), i.e. advancing faster than expected based on dispersal and growth at low densities. Genetic diversity is also lost at a slower rate in these expansions (**Fig. 4**), confirming again previous results about pushed expansions, which were however derived in landscapes with much larger population sizes, i.e. where drift and dispersal stochasticity were likely much less important. We also confirm that increasing the equilibrium population size *K* leads to faster range expansions, as previously shown by Haond et al. (2018).

In simulations, reducing connectedness also led to slower expansions (lower absolute speed v) that were also pushed (higher velocity ratio $\frac{v}{v_F}$, **Fig. 2**). Pushed expansions arise when there is positive-density dependency in dispersal and/or growth at least at lower densities (Birzu et al., 2019; Gandhi et al., 2016; Haond et al., 2018; Lewis et al., 2016)**.** This result confirms our main prediction that the positive relationship between population density and establishment probability **(Fig. 1)** arising at low population sizes when connectedness declines can be enough to generate pushed expansions.

In experimental landscapes, contrary to simulations, expansions advanced just as fast when connectedness was reduced (**Fig. 3**). Importantly, it does not mean that reducing connectedness does not lead to more pushed expansions, on the contrary. What differentiates between pushed and pulled expansions is not absolute velocity *v* (which can be either higher or lower in pushed expansions (Gandhi et al., 2019), **Fig. 2**), but the ratio to the "equivalent" pulled wave's velocity, so v/v_F. While we do not have direct quantitative information on the v_F of our experimental landscapes, we have some partial and indirect qualitative information. Indeed, a reduction of connectedness and thus dispersal implies by definition a reduction of v_F, growth being equal (see also **Supplementary**

Material 3). If $v_{[reference]} \approx v_{[reduced]}$ (**Fig. 3**) and $v_{F[reference]} > v_{F[reduced]}$, then it follows that $v_{[reference]} / v_{F[reference]} < v_{[reduced]} / v_{F[reduced]}$. This would mean that "reduced connectedness" expansions are indeed more pushed than reference expansions in our experiment. Our results thus show that full information about the density-dependency of growth or movement is not always needed to make qualitative assessments of the "pushiness" degree of a given expansion relative to a reference. This is particularly interesting for the study of biological invasions and range shifts in the wild, especially in (larger) organisms that are not easily reared and maintained in laboratory conditions. More work is needed to determine whether more quantitative insights can also be obtained from incomplete life-history and population dynamics data typical of "natural" study systems.

Mismatches to genetic diversity predictions show pushed expansion are more diverse than expected

A key theoretical prediction is that pushed expansions lose genetic diversity at a slower rate than comparable pulled expansions (Birzu et al., 2019; Hallatschek & Nelson, 2008; Roques et al., 2012). While our simulated pushed expansions generated by density-dependent dispersal or Allee effects conform to this prediction (**Fig. 4**), this is not the case for the ones we generated by reducing connectedness: these expansions lost genetic diversity slightly faster than the pulled reference (**Fig. 4**) despite being clearly "pushed" based on velocity ratios. This conflict between two definitions of pushed expansions is at first glance surprising, as previous theory implied changes in velocity and in genetic diversity dynamics were intrinsically correlated (e.g. Birzu et al., 2018). We can however solve this apparent contradiction in two steps. First, reducing connectedness, intuitively, does reduce the *absolute* number of individuals that start new populations (**Supplementary Material 7, Fig. 6**), which would intuitively lead to lower effective population sizes N_e and a faster decay of genetic diversity (Birzu et al., 2018, 2019; Hallatschek & Nelson, 2008). However, because more dispersal attempts stochastically fail at lower connectedness (**Fig. 1**), the *relative* number of individuals contributing to a new population (compared to the pulled and deterministic expectation) is actually higher when connectedness is reduced (**Supplementary Material 7, Fig. 6**), as expected from pushed expansions. When the first mechanism has a stronger impact on genetic diversity, we can expect to see expansions that are pushed yet lose more genetic diversity, as in our simulations.

In experimental landscapes, reducing connectedness did slow the decay of genetic diversity at the edge of the expansion (**Fig. 5**), as was expected from pushed expansion theory (Birzu et al., 2018, 2019; Gandhi et al., 2019; Roques et al., 2012). However, as seen above, this result contradicts simulations showing "pushed" expansions arising solely because of reduced connectedness should lose genetic diversity faster than the equivalent expansion with higher connectedness. The mismatch

between simulations and experiments regarding genetic diversity may indicate increased stochasticity is not the only mechanism at play here.

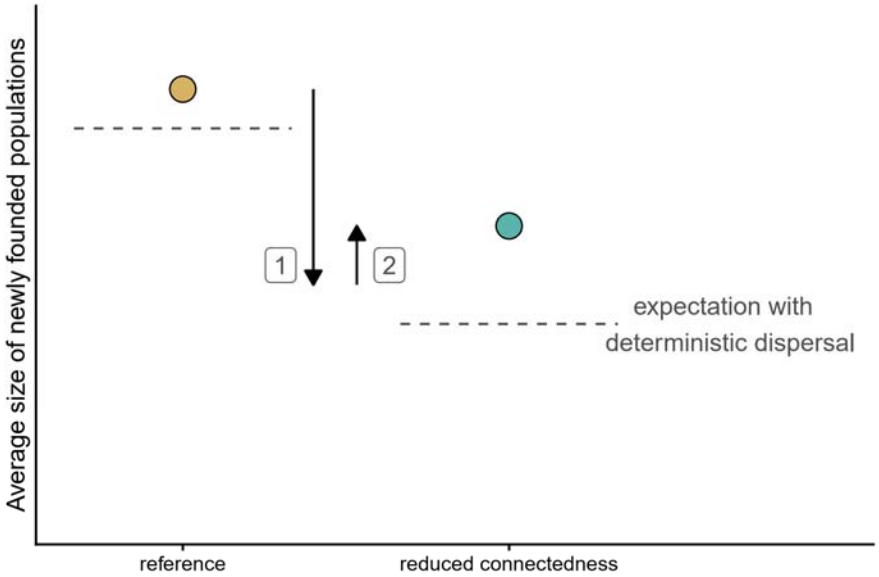

Figure 6. Conceptual model of how the effect of reduced connectedness on observed founding population size (dots) and ultimately genetic diversity can be separated into the effects of connectedness proper (smaller founding populations because fewer individuals reach new patches; arrow #1) and those of the shifts to more pushed dynamics (because of stochasticity, founding populations are larger than if dispersal was deterministic; arrow #2). Values on y-axis are not to scale and chosen for illustrative purposes only; statistical analyses underpinning this graphical summary are presented in **Supplementary Material 7**

First, dispersal decisions depend on the balance between costs and benefits of both dispersal and philopatry. While reducing connectedness increases the costs of dispersal (Bonte et al., 2012), leading to a decrease in dispersal (Benoit et al., 2020; Bonte et al., 2012), this effect may be weaker at higher densities, if costs associated with competition are strong enough to trigger dispersal anyway. Reduced connectedness would then strengthen the density-dependency of dispersal, leading to more pushed expansions through another mechanism. To test this verbal model, we implemented it in further range expansion simulations (**Supplementary Material 8**), adding a treatment combining reduced base dispersal and positive density-dependent dispersal at the same time. This treatment, in which dispersal at higher densities close to *K* is more or less the same than in reference expansions, results in simulated expansions that match our experiment better. Indeed, the

445 resulting expansions (i) are pushed based on velocity ratios (ii) have an absolute speed closer to
446 reference expansions than when only reduced connectedness is applied, and (iii) lose genetic
447 diversity slower. For this mechanism to plausibly apply to our experimental system, *Trichogramma*
448 wasps need to be able to detect when density and competition increase locally, and adjust their
449 spatial behaviour in response (which they do; Wajnberg, Fauvergue, & Pons, 2000).

450 In "small" populations such as the ones we studied here, more intense selection may reduce the
451 effective size N_e (Robertson, 1961), and thus accelerate the loss of neutral genetic diversity. While we
452 may expect selection by spatial sorting (Phillips & Perkins, 2019) to be weaker in pushed expansions
453 (as the spatial "filter" allows more individuals forward), this probably would not be the case in
454 pushed expansions caused by reduced connectedness. Indeed, increased landscape fragmentation is
455 on the contrary known to exert strong selective pressures on dispersal, and on the multiple traits
456 correlated with it (Cote et al., 2017). Direct analysis of phenotypic changes during expansions is
457 needed to disentangle the ways lower connectedness can influence diversity loss.

458 Finally, experimental landscapes with reduced connectedness may lose genetic diversity more slowly
459 simply because they exhibit larger populations, rather than due to a shift in regime from (more)
460 pulled to (more) pushed expansions. While we do find indications that equilibrium population sizes
461 were larger when connectedness was reduced (**Supplementary Material 9**), we do not believe it is
462 the main driver of our genetic diversity results. Indeed, if the differences in genetic dynamics at the
463 edge were mostly due to differences in carrying capacities *K*, we should then expect similar dynamics
464 in core populations, at least qualitatively (as seen **Fig. 4** for simulated results). This is not the case, as
465 genetic decay rates are not different between treatments in experimental core patches (**Fig. 5**).

466 ***Conclusion***

467 In this study, we demonstrated a new mechanism for generating pushed(-like) expansions (**Fig. 1**).
468 We showed that the genetic and velocity aspects of the pushed/pulled distinction, which have been
469 assumed to be tightly linked (Birzu et al., 2018) can be decoupled in these contexts. This is not
470 without precedent, as similar results have been found regarding front width and velocity (Gandhi et
471 al., 2016). This decoupling means (empirical) researchers investigating range expansions under the
472 pushed/pulled lens must be careful about which questions they ask and whether the dimensions of
473 "pushiness" they collect data on are the appropriate ones. More generally, this shows more studies
474 are needed to better characterize the different types of pushed expansions and their impacts. We
475 also showed pushed expansions can be detected and analysed in systems with (relatively) low
476 population sizes, even though theory has been developed on much higher population sizes. This

means the pushed-pulled framework is useful in a broad range of contexts and taxa, and may be valuable to help understand and better predict range expansions and shifts under natural conditions.

Finally, our experimental results show that, in some cases, reducing connectedness may limit the loss of genetic diversity while not substantially impeding spread rates. This leads to the somewhat counterintuitive conclusion that reducing connectivity may in some cases benefit expanding species (compare and contrast with e.g. Hodgson, Thomas, Dytham, Travis, & Cornell, 2012; Kinezaki, Kawasaki, & Shigesada, 2010). Given one of the main causes of pushed expansions, positive density-dependent dispersal, is frequent in nature (see syntheses in Harman et al., 2020; Matthysen, 2005), this has strong implications for the management of invasive species and species undergoing range shifts. Also, as density-dependent dispersal (Fronhofer, Gut, & Altermatt, 2017; Travis, Mustin, Benton, & Dytham, 2009) and Allee effects (Datta, Korolev, Cvijovic, Dudley, & Gore, 2013; Erm & Phillips, 2020) themselves may evolve during range expansions, and given the consequences of habitat fragmentation on dispersal ecology and evolution (Cote et al., 2017; Jacob, Laurent, Morel-Journel, & Schtickzelle, 2020; Travis, Smith, & Ranwala, 2010), we call for more systematic eco-evolutionary studies of context-dependent dynamics during range expansions and shifts.

Acknowledgements

We thank participants to the 2019 conference of the British Ecological Society for their helpful comments.

Data availability

Data, Netlogo model code and R scripts to reproduce all analyses presented in this manuscript are available on GitHub (https://github.com/mdahirel/pushed-pulled-2020-dynamics) and Zenodo (doi: 10.5281/zenodo.3969988).

Funding

This work was funded by the French Agence Nationale de la Recherche (TriPTIC, ANR-14-CE18-0002; PushToiDeLa, ANR-18-CE32-0008), and received funding from the European Union Seventh Framework Programme FP7 (grant agreement FP7-IAPP #324475 "COLBICS").

References

Baudry, J., & Merriam, H. G. (1987). Connectivity and connectedness: functional versus structural patterns in landscapes. In K.-F. Schreiber (Ed.), *Connectivity in Landscape Ecology* (pp. 23–28). Münster.

Benoit, L., Hewison, A. J. M., Coulon, A., Debeffe, L., Grémillet, D., Ducros, D., … Morellet, N. (2020). Accelerating across the landscape: The energetic costs of natal dispersal in a large herbivore. *Journal of Animal Ecology*, *89*(1), 173–185. doi: 10.1111/1365-2656.13098

Berec, L., Angulo, E., & Courchamp, F. (2007). Multiple Allee effects and population management. *Trends in Ecology & Evolution*, *22*(4), 185–191. doi: 10.1016/j.tree.2006.12.002

Birzu, G., Hallatschek, O., & Korolev, K. S. (2018). Fluctuations uncover a distinct class of traveling waves. *Proceedings of the National Academy of Sciences*, *115*(16), E3645–E3654. doi: 10.1073/pnas.1715737115

Birzu, G., Matin, S., Hallatschek, O., & Korolev, K. S. (2019). Genetic drift in range expansions is very sensitive to density dependence in dispersal and growth. *Ecology Letters*, *22*(11), 1817–1827. doi: 10.1111/ele.13364

Bonte, D., Van Dyck, H., Bullock, J. M., Coulon, A., Delgado, M., Gibbs, M., … Travis, J. M. J. (2012). Costs of dispersal. *Biological Reviews*, *87*(2), 290–312. doi: 10.1111/j.1469-185X.2011.00201.x

Bowler, D. E., & Benton, T. G. (2005). Causes and consequences of animal dispersal strategies: relating individual behaviour to spatial dynamics. *Biological Reviews*, *80*(2), 205–225. doi: 10.1017/S1464793104006645

Bürkner, P.-C. (2017). brms: an R package for bayesian multilevel models using Stan. *Journal of Statistical Software*, *80*(1), 1–28. doi: 10.18637/jss.v080.i01

Carpenter, B., Gelman, A., Hoffman, M. D., Lee, D., Goodrich, B., Betancourt, M., … Riddell, A. (2017). Stan: a probabilistic programming language. *Journal of Statistical Software*, *76*(1), 1–32. doi: 10.18637/jss.v076.i01

Cerutti, F., & Bigler, F. (1995). Quality assessment of *Trichogramma brassicae* in the laboratory. *Entomologia Experimentalis et Applicata*, *75*(1), 19–26. doi: 10.1111/j.1570-7458.1995.tb01905.x

Cote, J., Bestion, E., Jacob, S., Travis, J., Legrand, D., & Baguette, M. (2017). Evolution of dispersal strategies and dispersal syndromes in fragmented landscapes. *Ecography*, *40*(1), 56–73. doi: 10.1111/ecog.02538

Datta, M. S., Korolev, K. S., Cvijovic, I., Dudley, C., & Gore, J. (2013). Range expansion promotes cooperation in an experimental microbial metapopulation. *Proceedings of the National Academy of Sciences*, *110*(18), 7354–7359. doi: 10.1073/pnas.1217517110

De Meester, N., & Bonte, D. (2010). Information use and density-dependent emigration in an agrobiont spider. *Behavioral Ecology*, *21*(5), 992–998. doi: 10.1093/beheco/arq088

DeAngelis, D. L., & Mooij, W. M. (2005). Individual-based modeling of ecological and evolutionary processes. *Annual Review of Ecology, Evolution, and Systematics*, *36*, 147–168.

Endriss, S. B., Vahsen, M. L., Bitume, E. V., Monroe, J. G., Turner, K. G., Norton, A. P., & Hufbauer, R. A. (2019). The importance of growing up: juvenile environment influences dispersal of individuals and their neighbours. *Ecology Letters*, *22*(1), 45–55. doi: 10.1111/ele.13166

Erm, P., & Phillips, B. L. (2020). Evolution Transforms Pushed Waves into Pulled Waves. *The American Naturalist*, *195*(3), E87–E99. doi: 10.1086/707324

Facon, B., Genton, B. J., Shykoff, J., Jarne, P., Estoup, A., & David, P. (2006). A general eco-evolutionary framework for understanding bioinvasions. *Trends in Ecology & Evolution*, *21*(3), 130–135. doi: 10.1016/j.tree.2005.10.012

Fellous, S., Duncan, A., Coulon, A., & Kaltz, O. (2012). Quorum Sensing and Density-Dependent Dispersal in an Aquatic Model System. *PLoS ONE*, *7*(11), e48436. doi: 10.1371/journal.pone.0048436

Fronhofer, E. A., Gut, S., & Altermatt, F. (2017). Evolution of density-dependent movement during experimental range expansions. *Journal of Evolutionary Biology*, *30*(12), 2165–2176. doi: 10.1111/jeb.13182

Fronhofer, Emanuel A., Legrand, D., Altermatt, F., Ansart, A., Blanchet, S., Bonte, D., … Cote, J. (2018). Bottom-up and top-down control of dispersal across major organismal groups. *Nature Ecology & Evolution*, *2*(12), 1859. doi: 10.1038/s41559-018-0686-0

Gabry, J., Simpson, D., Vehtari, A., Betancourt, M., & Gelman, A. (2019). Visualization in Bayesian workflow. *Journal of the Royal Statistical Society: Series A (Statistics in Society)*, *182*(2), 389–402. doi: 10.1111/rssa.12378

Gandhi, S. R., Korolev, K. S., & Gore, J. (2019). Cooperation mitigates diversity loss in a spatially expanding microbial population. *Proceedings of the National Academy of Sciences*, *116*(47), 23582–23587. doi: 10.1073/pnas.1910075116

Gandhi, S. R., Yurtsev, E. A., Korolev, K. S., & Gore, J. (2016). Range expansions transition from pulled to pushed waves as growth becomes more cooperative in an experimental microbial population. *Proceedings of the National Academy of Sciences*, *113*(25), 6922–6927. doi: 10.1073/pnas.1521056113

Hallatschek, O., & Nelson, D. R. (2008). Gene surfing in expanding populations. *Theoretical Population Biology*, *73*(1), 158–170. doi: 10.1016/j.tpb.2007.08.008

Haond, M., Morel-Journel, T., Lombaert, E., Vercken, E., Mailleret, L., & Roques, L. (2018). When higher carrying capacities lead to faster propagation. *BioRxiv (Peer-Reviewed and Recommended by Peer Community In Ecology)*, 307322. doi: 10.1101/307322

Harman, R. R., Ii, J. G., Shivaji, R., & Cronin, J. T. (2020). Frequency of occurrence and population-dynamic consequences of different forms of density-dependent emigration. *The American Naturalist*, *195*(5), 851–867. doi: 10.1086/708156

Hastings, A., Cuddington, K., Davies, K. F., Dugaw, C. J., Elmendorf, S., Freestone, A., … Thomson, D. (2005). The spatial spread of invasions: new developments in theory and evidence. *Ecology Letters*, *8*(1), 91–101. doi: 10.1111/j.1461-0248.2004.00687.x

Hill, J. K., Griffiths, H. M., & Thomas, C. D. (2011). Climate change and evolutionary adaptations at species' range margins. *Annual Review of Entomology*, *56*(1), 143–159. doi: 10.1146/annurev-ento-120709-144746

Hodgson, J. A., Thomas, C. D., Dytham, C., Travis, J. M. J., & Cornell, S. J. (2012). The speed of range shifts in fragmented landscapes. *PLOS ONE*, *7*(10), e47141. doi: 10.1371/journal.pone.0047141

Jacob, S., Chaine, A. S., Huet, M., Clobert, J., & Legrand, D. (2019). Variability in dispersal syndromes is a key driver of metapopulation dynamics in experimental microcosms. *The American Naturalist*, *194*(5), 613–626. doi: 10.1086/705410

Jacob, S., Laurent, E., Morel-Journel, T., & Schtickzelle, N. (2020). Fragmentation and the context-dependence of dispersal syndromes: matrix harshness modifies resident-disperser phenotypic differences in microcosms. *Oikos*, *129*(2), 158–169. doi: 10.1111/oik.06857

Jombart, T. (2008). adegenet: a R package for the multivariate analysis of genetic markers. *Bioinformatics*, *24*(11), 1403–1405. doi: 10.1093/bioinformatics/btn129

Kay, M. (2019). *tidybayes: Tidy Data and Geoms for Bayesian Models*. doi: 10.5281/zenodo.1308151

Kinezaki, N., Kawasaki, K., & Shigesada, N. (2010). The effect of the spatial configuration of habitat fragmentation on invasive spread. *Theoretical Population Biology*, *78*(4), 298–308. doi: 10.1016/j.tpb.2010.09.002

Krauss, J., Steffan-Dewenter, I., & Tscharntke, T. (2003). How does landscape context contribute to effects of habitat fragmentation on diversity and population density of butterflies? *Journal of Biogeography*, *30*(6), 889–900. doi: 10.1046/j.1365-2699.2003.00878.x

Kruschke, J. (2015). *Doing Bayesian Data Analysis: A Tutorial with R, JAGS, and Stan* (2nd ed.). Boston: Academic Press.

Kuefler, D., Avgar, T., & Fryxell, J. M. (2012). Rotifer population spread in relation to food, density and predation risk in an experimental system: *State-dependent rate of population spread*. *Journal of Animal Ecology*, *81*(2), 323–329. doi: 10.1111/j.1365-2656.2011.01917.x

Larsen, C. D., & Hargreaves, A. L. (2020). Miniaturizing landscapes to understand species distributions. *Ecography*, *43*(n/a). doi: 10.1111/ecog.04959

Lavergne, S., Mouquet, N., Thuiller, W., & Ronce, O. (2010). Biodiversity and climate change: integrating evolutionary and ecological responses of species and communities. *Annual Review of Ecology, Evolution, and Systematics*, *41*(1), 321–350. doi: 10.1146/annurev-ecolsys-102209-144628

Lewis, M., Petrovskii, S. V., & Potts, J. (2016). *The Mathematics Behind Biological Invasions*. doi: 10.1007/978-3-319-32043-4

Marjamäki, P. H., Contasti, A. L., Coulson, T. N., & McLoughlin, P. D. (2013). Local density and group size interacts with age and sex to determine direction and rate of social dispersal in a polygynous mammal. *Ecology and Evolution*, *3*(9), 3073–3082. doi: 10.1002/ece3.694

Matthysen, E. (2005). Density-dependent dispersal in birds and mammals. *Ecography*, *28*(3), 403–416.

McElreath, R. (2020). *Statistical Rethinking: A Bayesian Course with Examples in R and Stan* (2nd edition). Boca Raton: Chapman and Hall/CRC.

Morel-Journel, T., Girod, P., Mailleret, L., Auguste, A., Blin, A., & Vercken, E. (2016). The highs and lows of dispersal: how connectivity and initial population size jointly shape establishment dynamics in discrete landscapes. *Oikos*, *125*(6), 769–777. doi: 10.1111/oik.02718

Nei, M. (1973). Analysis of gene diversity in subdivided populations. *Proceedings of the National Academy of Sciences*, *70*(12), 3321–3323. doi: 10.1073/pnas.70.12.3321

Pachepsky, E., & Levine, J. M. (2011). Density Dependence Slows Invader Spread in Fragmented Landscapes. *The American Naturalist*, *177*(1), 18–28. doi: 10.1086/657438

Parmesan, C. (2006). Ecological and evolutionary responses to recent climate change. *Annual Review of Ecology, Evolution, and Systematics*, *37*(1), 637–669. doi: 10.1146/annurev.ecolsys.37.091305.110100

Pedersen, T. L. (2019). *patchwork: The Composer of Plots*. Retrieved from https://CRAN.R-project.org/package=patchwork

Phillips, B. L., & Perkins, T. A. (2019). Spatial sorting as the spatial analogue of natural selection. *Theoretical Ecology*. doi: 10.1007/s12080-019-0412-9

R Core Team. (2020). R: a language and environment for statistical computing (Version 4.0.0). Retrieved from https://www.R-project.org/

Renault, D., Laparie, M., McCauley, S. J., & Bonte, D. (2018). Environmental adaptations, ecological filtering, and dispersal central to insect invasions. *Annual Review of Entomology*, *63*(1), 345–368. doi: 10.1146/annurev-ento-020117-043315

Robertson, A. (1961). Inbreeding in artificial selection programmes. *Genetics Research*, *2*, 189–194. doi: 10.1017/S0016672308009452

Roques, L., Garnier, J., Hamel, F., & Klein, E. K. (2012). Allee effect promotes diversity in traveling waves of colonization. *Proceedings of the National Academy of Sciences*, *109*(23), 8828–8833. doi: 10.1073/pnas.1201695109

Salecker, J., Sciaini, M., Meyer, K. M., & Wiegand, K. (2019). The nlrx r package: A next-generation framework for reproducible NetLogo model analyses. *Methods in Ecology and Evolution*, *10*(11), 1854–1863. doi: 10.1111/2041-210X.13286

Santini, L., Isaac, N. J. B., & Ficetola, G. F. (2018). TetraDENSITY: A database of population density estimates in terrestrial vertebrates. *Global Ecology and Biogeography*, *27*(7), 787–791. doi: 10.1111/geb.12756

Sexton, J. P., McIntyre, P. J., Angert, A. L., & Rice, K. J. (2009). Evolution and ecology of species range limits. *Annual Review of Ecology, Evolution, and Systematics*, *40*(1), 415–436. doi: 10.1146/annurev.ecolsys.110308.120317

Stan Development Team. (2018). RStan: the R interface to Stan (Version 2.17.3). Retrieved from http://mc-stan.org

Stevens, V. M., Trochet, A., Blanchet, S., Moulherat, S., Clobert, J., & Baguette, M. (2013). Dispersal syndromes and the use of life-histories to predict dispersal. *Evolutionary Applications*, *6*(4), 630–642. doi: 10.1111/eva.12049

Stokes, A. N. (1976). On two types of moving front in quasilinear diffusion. *Mathematical Biosciences*, *31*(3), 307–315. doi: 10.1016/0025-5564(76)90087-0

St-Onge, M., Cormier, D., Todorova, S., & Lucas, É. (2014). Comparison of *Ephestia* kuehniella eggs sterilization methods for *Trichogramma* rearing. *Biological Control*, *70*, 73–77. doi: 10.1016/j.biocontrol.2013.12.006

Travis, J. M. J., Mustin, K., Benton, T. G., & Dytham, C. (2009). Accelerating invasion rates result from the evolution of density-dependent dispersal. *Journal of Theoretical Biology*, *259*(1), 151–158. doi: 10.1016/j.jtbi.2009.03.008

Travis, J. M. J., Smith, H. S., & Ranwala, S. M. W. (2010). Towards a mechanistic understanding of dispersal evolution in plants: conservation implications. *Diversity and Distributions*, *16*(4), 690–702. doi: 10.1111/j.1472-4642.2010.00674.x

Van Allen, B. G., & Bhavsar, P. (2014). Natal habitat effects drive density—dependent scaling of dispersal decisions. *Oikos*, *123*(6), 699–704. doi: 10.1111/oik.01240

Van Petegem, K., Moerman, F., Dahirel, M., Fronhofer, E. A., Vandegehuchte, M. L., Van Leeuwen, T., … Bonte, D. (2018). Kin competition accelerates experimental range expansion in an arthropod herbivore. *Ecology Letters*, *21*(2), 225–234. doi: 10.1111/ele.12887

Vehtari, A., Gelman, A., Simpson, D., Carpenter, B., & Bürkner, P.-C. (2020). Rank-normalization, folding, and localization: An improved \widehat{R} for assessing convergence of MCMC. *Bayesian Analysis*. doi: 10.1214/20-BA1221

Wajnberg, E., Fauvergue, X., & Pons, O. (2000). Patch leaving decision rules and the Marginal Value Theorem: an experimental analysis and a simulation model. *Behavioral Ecology*, *11*(6), 577–586. doi: 10.1093/beheco/11.6.577

Walter, J. A., Grayson, K. L., Blackburn, L. M., Tobin, P. C., & Johnson, D. M. (2019). Spatiotemporal variability in Allee effects of invading gypsy moth populations. *Biological Invasions*. doi: 10.1007/s10530-019-02096-5

Wickham, H., Averick, M., Bryan, J., Chang, W., McGowan, L., François, R., … Yutani, H. (2019). Welcome to the Tidyverse. *Journal of Open Source Software*, *4*(43), 1686. doi: 10.21105/joss.01686

Wilensky, U. (1999). *NetLogo*. Retrieved from http://ccl.northwestern.edu/netlogo/

Williams, J. L., & Levine, J. M. (2018). Experimental evidence that density dependence strongly influences plant invasions through fragmented landscapes. *Ecology*, *99*(4), 876–884. doi: 10.1002/ecy.2156

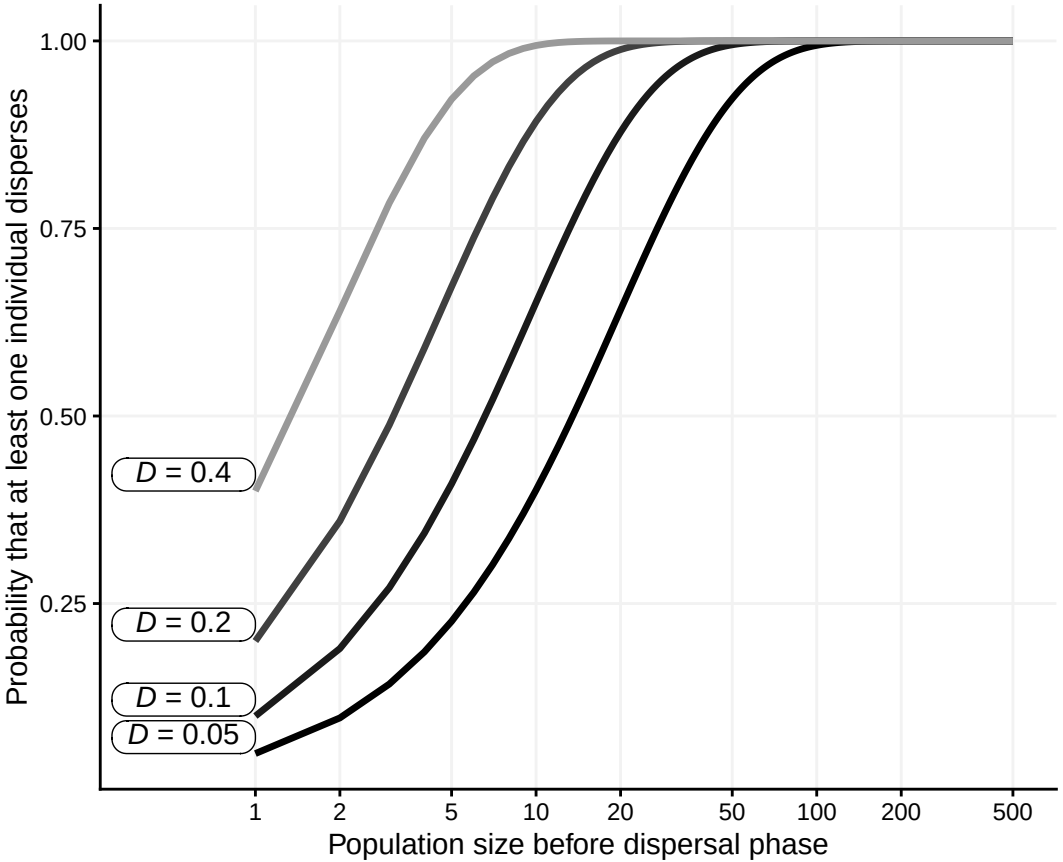
1.00
0.75
0.50
0.25
Probability that at least one individual disperses
D = 0.4
D = 0.2
D = 0.1
D = 0.05
1
2
5
10
20
50
100
200
500
Population size before dispersal phase

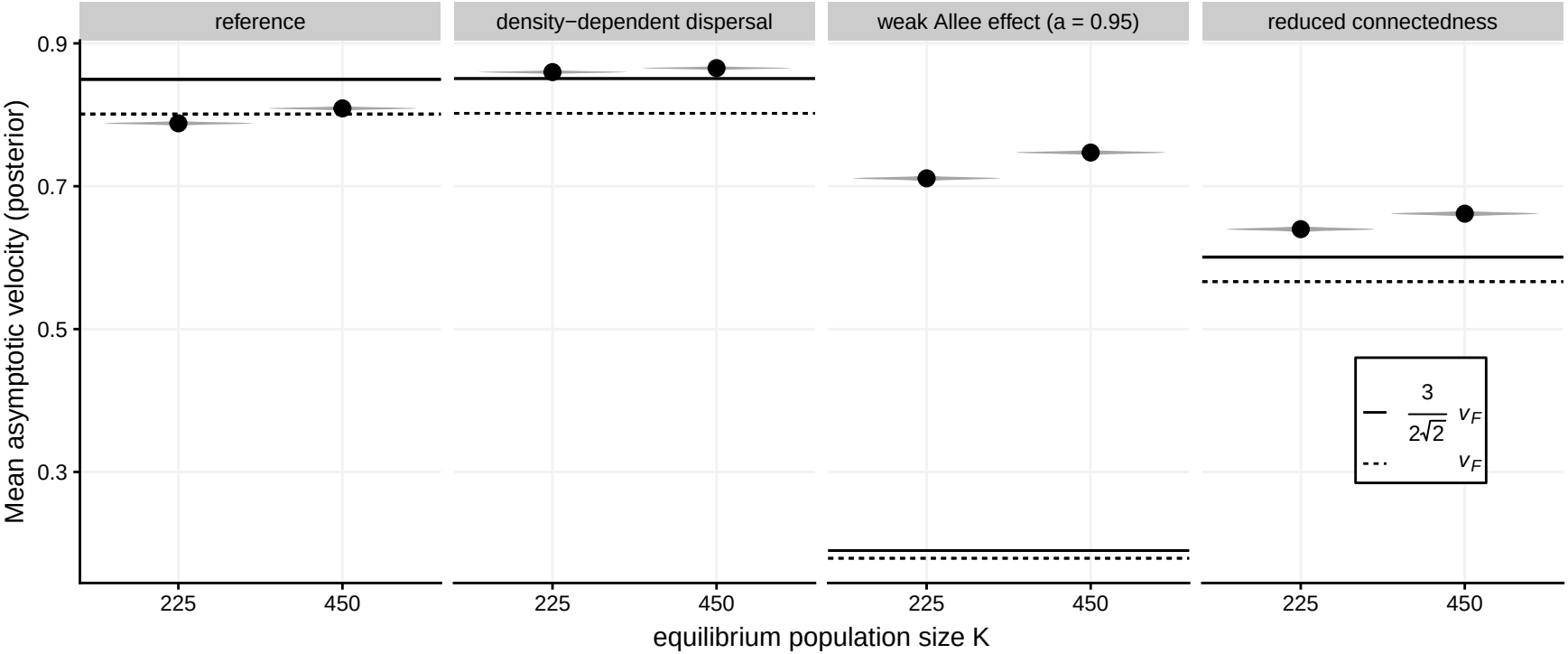
reference
density−dependent dispersal
weak Allee effect (a = 0.95)
reduced connectedness
Mean asymptotic velocity (posterior)
0.9
0.7
0.5
0.3
225
450
equilibrium population size K
$\frac{3}{2\sqrt{2}} v_F$
v_F

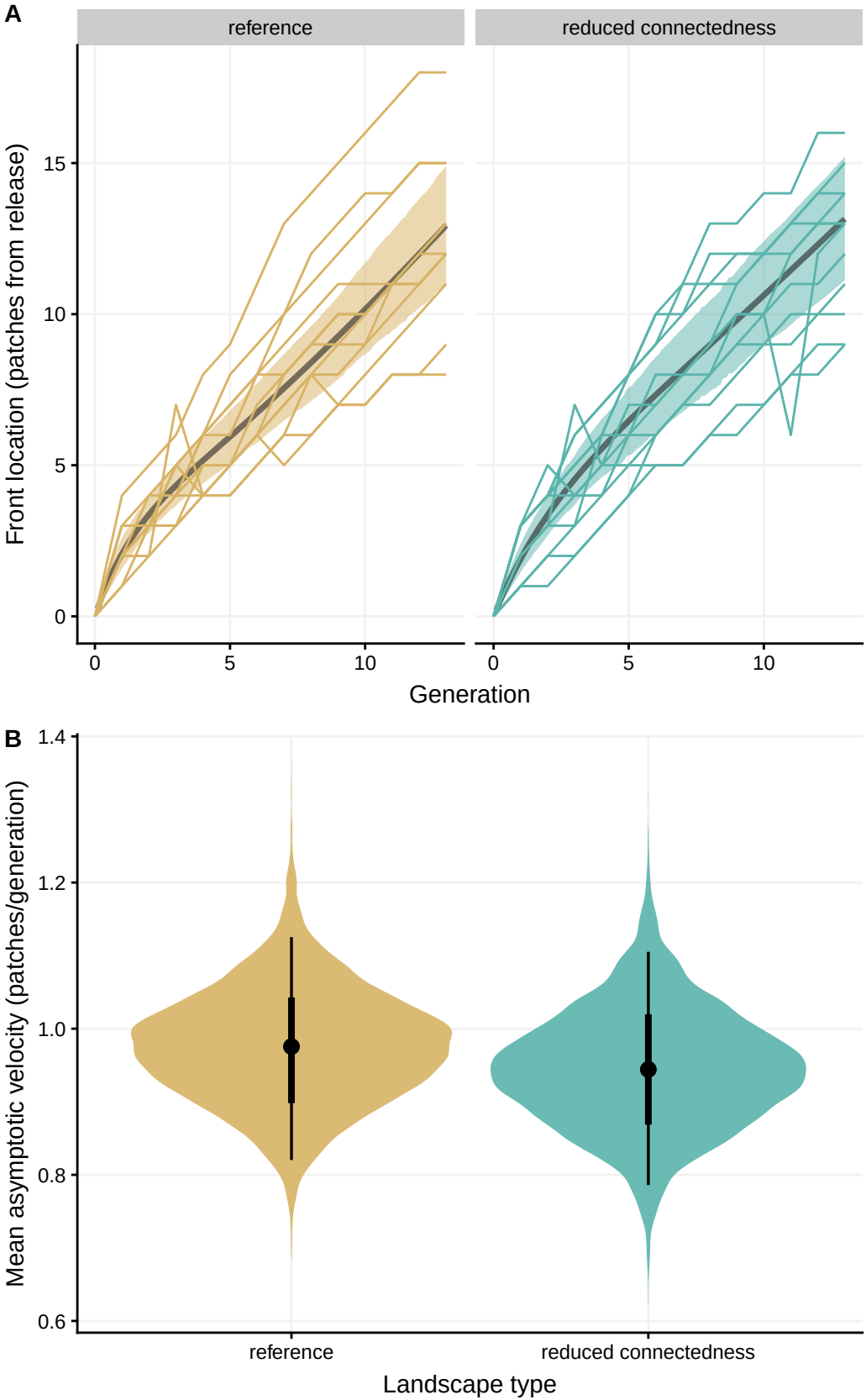
A
reference
reduced connectedness
Front location (patches from release)
0
5
10
15
0
5
10
0
5
10
Generation
B
Mean asymptotic velocity (patches/generation)
0.6
0.8
1.0
1.2
1.4
reference
reduced connectedness
Landscape type

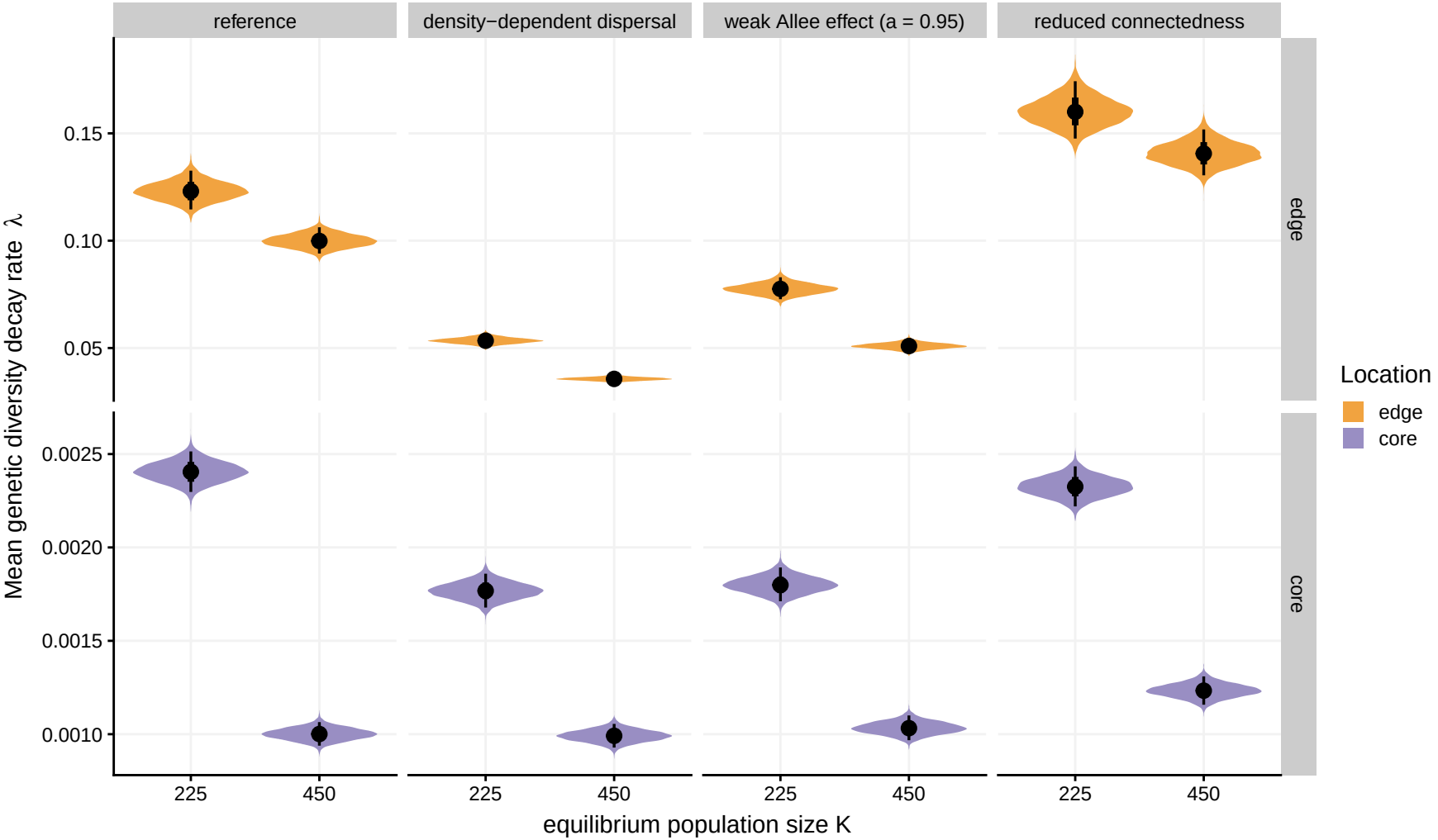
reference
density−dependent dispersal
weak Allee effect (a = 0.95)
reduced connectedness
edge
core
Mean genetic diversity decay rate λ
0.15
0.10
0.05
0.0025
0.0020
0.0015
0.0010
225
450
equilibrium population size K
Location
edge
core

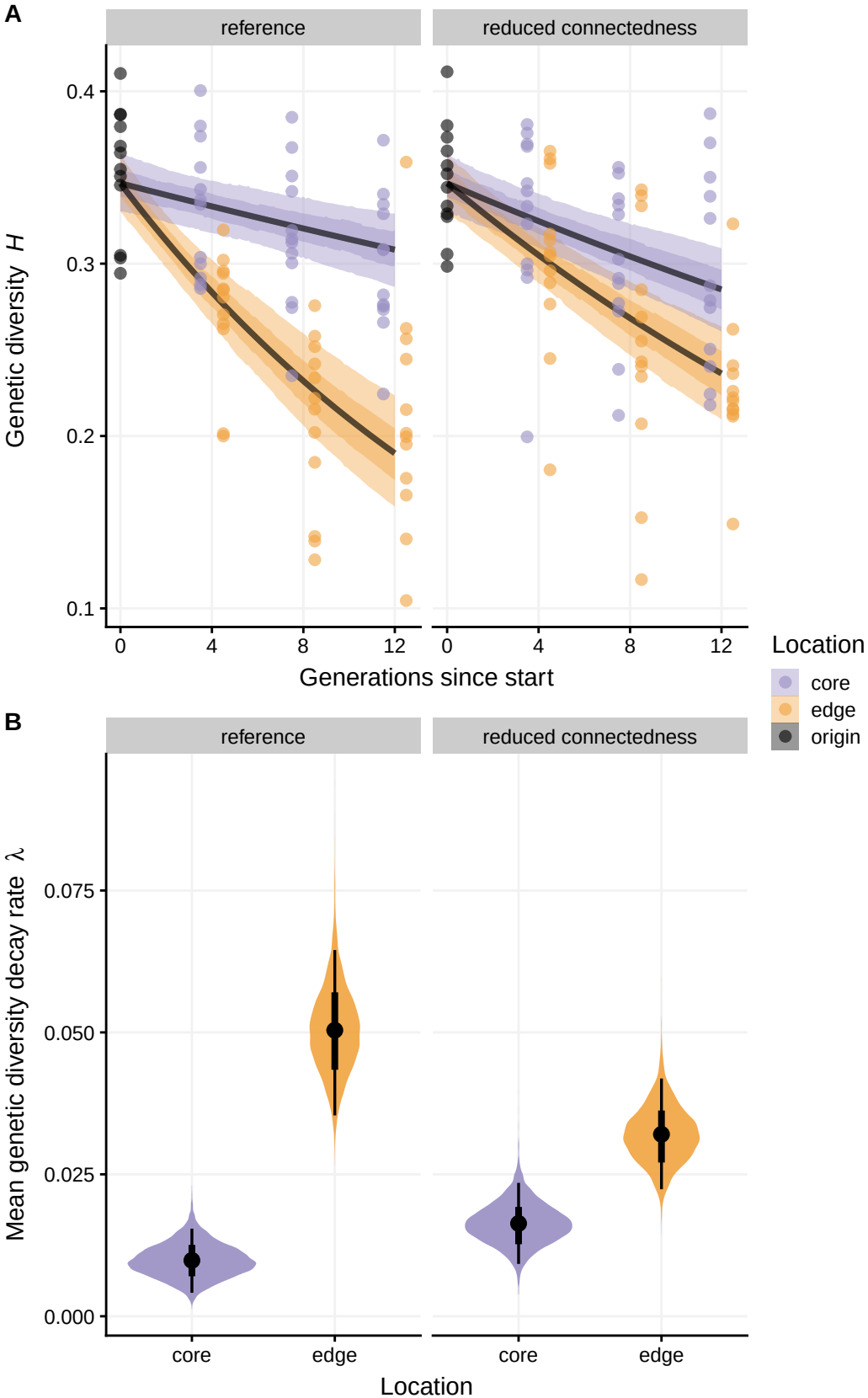
A
reference
reduced connectedness
Genetic diversity H
0.4
0.3
0.2
0.1
0
4
8
12
Generations since start
Location
core
edge
origin
B
reference
reduced connectedness
Mean genetic diversity decay rate λ
0.075
0.050
0.025
0.000
core
edge
Location

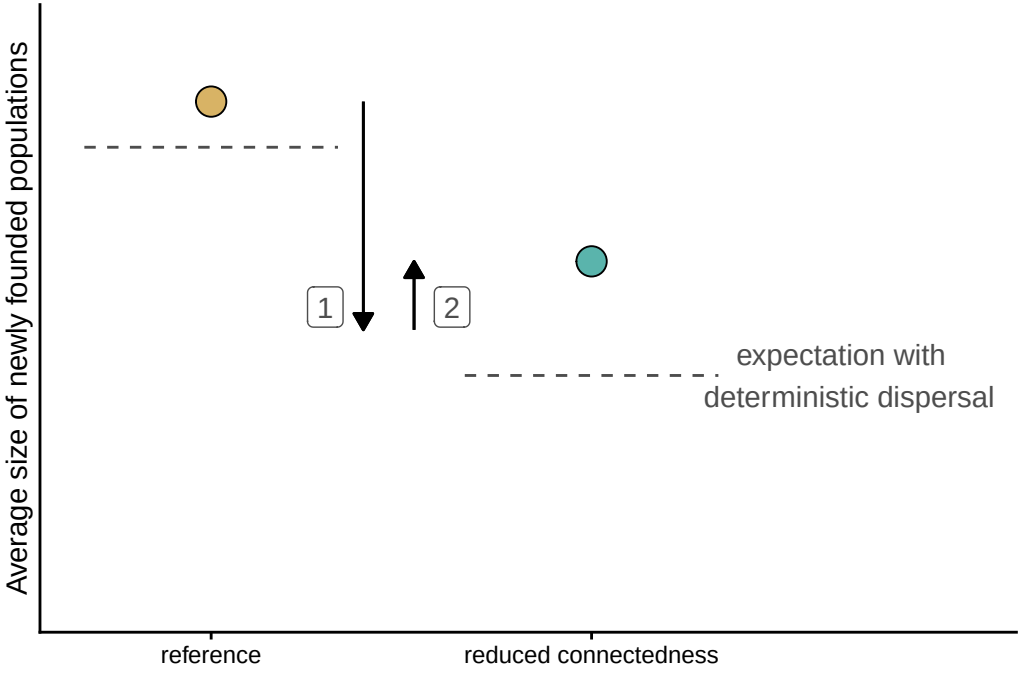
Average size of newly founded populations
1
2
expectation with
deterministic dispersal
reference
reduced connectedness